

# Testing New Physics Explanations of MiniBooNE Anomaly at Neutrino Scattering Experiments

Carlos A. Argüelles,<sup>1,\*</sup> Matheus Hostert,<sup>2,†</sup> and Yu-Dai Tsai<sup>3,‡</sup>

<sup>1</sup>*Dept. of Physics, Massachusetts Institute of Technology, Cambridge, MA 02139, USA*

<sup>2</sup>*Institute for Particle Physics Phenomenology, Department of Physics, Durham University, South Road, Durham DH1 3LE, United Kingdom*

<sup>3</sup>*Fermilab, Fermi National Accelerator Laboratory, Batavia, IL 60510, USA*

(Dated: December 21, 2018)

Testable neutrino mass generation models have recently been proposed as a solution to the MiniBooNE excess. In this article, we show how neutrino scattering experiments, such as MINER $\nu$ A and CHARM-II, can probe this class of models. We argue that by using sideband measurements of neutrino-electron scattering, we can significantly explore the parameter space motivated by the MiniBooNE results. Our new constraints show that a simultaneous explanation of the angular and energy distributions of the excess is in tension with neutrino-electron scattering data. We also provide an outlook of upcoming measurements that could further probe the new physics models of interest. In the context of those future measurements, we highlight the importance of control samples and improved theoretical understanding of neutrino-nucleus cross sections in the search for new physics in neutrino experiments.

**Introduction** – Non-zero neutrino masses have been established in the last twenty years by measurements of neutrino flavor conversion in natural and human-made sources, including long- and short-baseline experiments. The overwhelming majority of data points towards a three-neutrino framework. Within this framework, we have measured the mixing angles that parametrize the relationship between mass and flavor eigenstates to a level of precision in the range of ten percent [1]. The remaining unknowns are the absolute scale of neutrino masses and their origin, the CP-violating phase, and the mass ordering of the neutrino states. In addition, anomalies in short-baseline accelerator and reactor experiments [2–5] are yet to have satisfying explanations. The most significant anomalies are beyond statistical doubt. Minimal extensions of the three-neutrino framework to explain the anomalies introduce the so-called sterile neutrino states, which do not participate in Standard Model (SM) interactions in order to agree with measurements of the Z-boson invisible decay width [6]. Unfortunately, these minimal scenarios are disfavoured as they fail to explain all data [7–9]. This has led the community to explore nonminimal scenarios. Along this direction, it is interesting to study well-motivated neutrino-mass models that can also explain the short-baseline anomalies and are testable in the laboratory. In this work, we will examine the class of neutrino-mass-related models that have been proposed as an explanation of the anomalous observation of electron-neutrino-like events in MiniBooNE (MB) [5].

The MB excess is currently at  $4.7\sigma$  tension with the standard three-neutrino prediction [5]. While it is pos-

sible that the excess is fully or partially due to systematic uncertainties or SM backgrounds (see, *e.g.*, [10–12]), many Beyond the Standard Model (BSM) explanations have been put forth. These new physics (NP) scenarios typically require the existence of new particles, which can: participate in short-baseline oscillations [13–35], change the neutrino propagation in matter [32, 36], be produced in the beam or in the detector and its surroundings [37–44]. These models either increase the conversion of muon- to electron-neutrinos or produce electron-neutrino-like signatures in the detector, where in the latter category one typically exploits the fact that the LSND and MiniBooNE are Cherenkov detectors that cannot distinguish between electrons and photons. Although it is possible to consider MiniBooNE explanations that have little to no theoretical motivation, recent models [45–47] are motivated by neutrino-mass generation via hidden interactions in the heavy neutrino sector. In particular, the common feature of these models is the upscattering into a heavy neutrino, usually with tens to hundreds of MeV in mass, which subsequently decays into a pair of electrons. If collimated, this pair of electrons can fake a single electron signature.

In this article, we introduce new techniques to probe these testable neutrino mass generation models in past, present, and future neutrino experiments. In addition, our analysis showcases a generic way to look for models that rely on the ambiguity between photons and electrons to explain the MiniBooNE observation. Due to the electron-like nature of the excess, we consider neutrino-electron scattering measurements [48–52]. Although these experiments have been shown to provide powerful constraints on light new physics [53–55], the unique topology of the signatures we consider require us to go beyond the final processed sample quoted by the experiments and develop new ways to search for them. Since the typical heavy neutrino mass is in the hundreds-of-MeV regime, we focus on two high-energy neutrino

---

\* caad@mit.edu

† matheus.hostert@durham.ac.uk

‡ ystai@fnal.gov

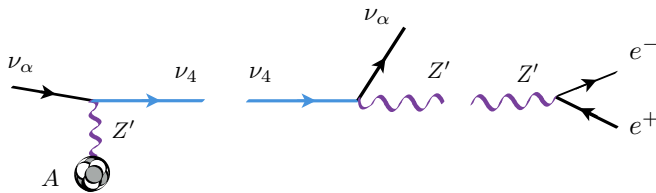


FIG. 1. *Illustration of heavy neutrino production.* Left: production of the heavy mass state via upscattering. Center: Decay of the heavy neutrino into a light neutrino and a gauge boson. Right: Decay of a gauge boson into a pair of electrons that produce the experimental signature.

experiments: MINER $\nu$ A [51, 56, 57] and CHARM-II [52, 58, 59]. These experiments are complementary in the range of neutrino energies they cover and have different background composition. In both cases we make use of sideband measurements, taking advantage of the excellent particle reconstruction capabilities of MINER $\nu$ A and the precise measurements at CHARM-II to constrain new physics. **Model** – We limit our discussion to the minimal version of the model that could explain the MB excess. This contains at least one heavy neutrino,  $\nu_D$ , charged under a new  $U(1)'$  gauge group, which is part of the particle content and gauge structure needed for mass generation. The dark sector is connected to the SM in two ways: through kinetic mixing between the new gauge boson and hypercharge, and through neutrino mass mixing. We start by specifying the kinetic part of the new physics Lagrangian

$$\mathcal{L}_{\text{kin}} \supset \frac{1}{4} \hat{Z}'_{\mu\nu} \hat{Z}'^{\mu\nu} + \frac{\sin \chi}{2} \hat{Z}'_{\mu\nu} \hat{B}^{\mu\nu} + \frac{m_{\hat{Z}'}^2}{2} \hat{Z}'^\mu \hat{Z}'_\mu, \quad (1)$$

where  $\hat{Z}'^\mu$  stands for the new gauge boson field,  $\hat{Z}'^{\mu\nu}$  is the field strength, and  $\hat{B}^{\mu\nu}$  the hypercharge field strength. After usual field redefinitions [60], we arrive at the physical states of the theory. Working at leading order in  $\chi$  and assuming  $m_{\hat{Z}'}^2/m_Z^2$  to be small, we can fully specify the relevant interaction Lagrangian as

$$\mathcal{L}_{\text{int}} \supset g_D \bar{\nu}_D \gamma_\mu \nu_D Z'^\mu + e \varepsilon Z'^\mu J_\mu^{\text{EM}}, \quad (2)$$

where  $J_\mu^{\text{EM}}$  is the SM electromagnetic current,  $g_D$  is the  $U(1)'$  gauge coupling assumed to be  $\mathcal{O}(1)$ , and  $\varepsilon \equiv c_w \chi$ , with  $c_w$  being the cosine of the weak angle. Note that additional terms would be present at higher orders in  $\chi$  and that mass mixing with the SM  $Z$  is also possible, though severely constrained. After electroweak symmetry breaking, the dark neutrino  $\nu_D$  is a superposition of SM neutrino mass states described by a  $4 \times 4$  unitary matrix  $U$ . In general, this matrix connects the flavor to the mass eigenstates  $\nu_i$  via

$$\nu_\alpha = \sum_{i=1}^4 U_{\alpha i} \nu_i, \quad (\alpha = e, \mu, \tau, D). \quad (3)$$

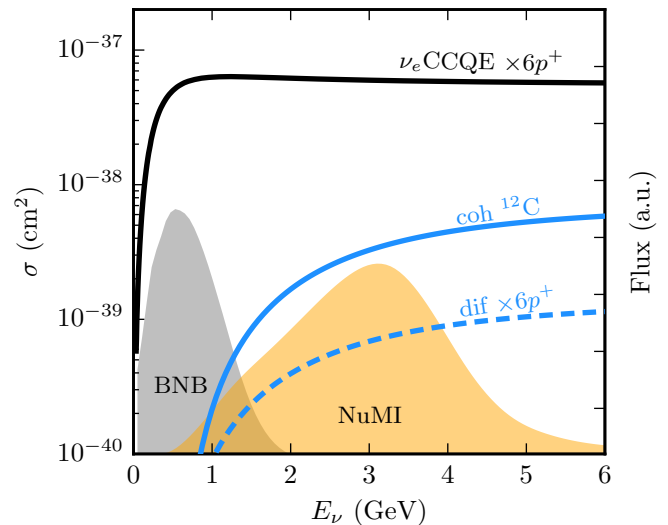


FIG. 2. *Upscattering cross section compared to the quasi-elastic.* The quasi-elastic cross section for  $6p^+$  is shown as a function of the neutrino energy (solid black line). Similarly the coherent, out of a carbon atom, and the diffractive new physics contributions for the benchmark point of [45] are shown as solid and dashed blue lines, respectively. In the background, the light gray shaded region is the Booster Neutrino Beam (BNB) flux shape, while the light golden region is the Neutrinos at the Main Injector (NuMI) low-energy neutrino-mode flux.

It is expected that  $|U_{\alpha 4}|$  is small for  $\alpha = e, \mu, \tau$ , but  $|U_{D4}|$  can be of  $\mathcal{O}(1)$  [7, 61]. The choice of  $m_4$  and  $m_{Z'}$  has important consequences for the allowed decays of the new particle content. We focus on the case in which  $m_4 > m_{Z'}$ , where the two body  $\nu_4 \rightarrow \nu_\alpha Z'$  decay is allowed. In addition, the mass of the new gauge boson is kept below  $\sim 100$  MeV, making the decay into  $e^+e^-$  pairs the dominant channel. Decay into a pair of neutrinos is possible, but is subdominant provided the mixing is small.

**Signature** – As illustrated in Fig. 1, the heavy neutrino is produced by upscattering from an active neutrino flavor state. The production cross section is proportional to  $\alpha_D \alpha_{\text{QED}} \varepsilon^2 |U_{\alpha 4}|^2$ , which is usually dominated by the muon-neutrino contribution due to the flavor composition of the beam. This production can happen off the whole nucleus in a coherent way or off individual nucleons. For  $m_{Z'} \lesssim 100$  MeV, the production will be mainly coherent, but for heavier masses, such as the ones considered in [47], the upscattering happens predominantly in a diffractive regime. In Fig. 2, we show the cross section at the benchmark point of [46] and compare it with the quasi-elastic cross section. By superimposing the cross section on the neutrino fluxes of MINER $\nu$ A and MiniBooNE, we make it explicit that the larger energies at MINER $\nu$ A and CHARM-II are ideal to probe these models. Once produced,  $\nu_4$  is then expected to decay promptly inside of the detector, setting a requirement on

its lifetime. The mass of the heavy neutrino also controls the angular distribution of the signal with respect to the beam. The lighter  $\nu_4$  is, the more forward the signal tends to be. The produced  $Z'$  is required to decay into an overlapping  $e^+e^-$  pair. The small opening angle of the overlapping pair required for it to be an explanation of MB excess sets the  $Z'$  mass to be at MeV scale. To summarize, increasing  $m_{Z'}$  has two effects. On one hand, it increases the ratio of diffractive to coherent upscattering, and on the other hand, it makes the electron pair less collimated. Even though we focus on overlapping  $e^+e^-$  pairs, we note that a significant fraction of events would appear as well-separated electrons or as a pair of electrons with large energy asymmetry, similarly to the neutral current  $\pi^0$  events. The asymmetric events also contribute to the MB excess and can also be looked for in  $\nu - e$  scattering analyses.

**Analysis** – Neutrino-electron scattering measurements at MINER $\nu$ A and CHARM-II predicate their cuts in the following core ideas: no hadronic activity near interaction vertex, small opening angle from the beam,  $E_e\theta^2 < 2m_e$ , and the measured energy deposition  $dE/dx$  needs to be consistent with that of a single electron. When the coherent process dominates and the mass of the  $Z'$  is small, the first two conditions are satisfied. However, the requirement of a single-electron-like energy deposition removes a significant fraction of the new-physics induced events. This presents a challenge, as the signal events are mostly overlapping electron pairs and will potentially be removed by the  $dE/dx$  cut. In order to circumvent this problem, we do our analysis not at the final-cut level, but at an intermediate one. The CHARM-II experiment provides data as a function of  $E_e\theta^2$  without the  $dE/dx$  cut, and in the case of MINER $\nu$ A we have access to the data as a function of the measured  $dE/dx$  after analysis cuts on  $E_e\theta^2$ .

We briefly describe the main features of the MINER $\nu$ A event selection here (for more details see [56]). The minimum electron energy required is 0.8 GeV. This threshold is placed in order to remove the  $\pi_0$  background and have reliable angular and energy reconstruction. Events are kept only when they meet the following angular separation criterion:  $E_e\theta^2 < 3.2 \times 10^{-3}$  GeV rad<sup>2</sup>. A final cut is applied, ensuring  $dE/dx < 4.5$  MeV/1.7 cm. The MINER $\nu$ A analysis uses the data outside the previous  $dE/dx$  cut to constrain backgrounds. This sideband is defined as all events with  $E_e\theta^2 > 5 \times 10^{-3}$  GeV rad<sup>2</sup> and  $dE/dx < 20$  MeV/1.7 cm. Using this sideband measurement, the collaboration tunes their backgrounds by (0.76, 0.64, 1.0) for ( $\nu_e$ CCQE,  $\nu_\mu$ NC,  $\nu_\mu$ CCQE) processes. We perform our analysis with the data shown in Fig. 3 of [56] where all the cuts are applied except for the final  $dE/dx$  cut. We have developed our own Monte Carlo (MC) to simulate candidate electron pair events; in our MC simulation, detector-resolution effects are assumed to be Gaussian with appropriate widths taken from [62]. We only consider the coherent part of the cross section to avoid hadronic-activity cuts, which is conservative. We

also select only events with small energy asymmetries and small opening electron angles. We calculate the mean  $dE/dx$  in plastic scintillators [63] according to [64, 65]. In our final event selection, we require that the sum of the energy deposited by each electron be more than 4.5 MeV/1.7 cm, which yields an efficiency of 90%. We obtain the expected size of neutrino-electron scattering and background events in this range from Fig. 3 of [56]. To place our limits, we perform a rate-only analysis by means of a  $\chi^2$  test statistic. We incorporate uncertainties in background size and flux normalization as nuisance parameters with Gaussian constrain terms. For the neutrino electron scattering and BSM signal, we allow the normalization to scale proportional to the same flux uncertainty parameter. The background term also scales with the flux-uncertainty parameter, but has an additional nuisance parameter to account for its unknown size. We obtain our constraint as a function of heavy neutrino mass  $m_4$ , and mixing  $|U_{\mu 4}|$  assuming with two degrees of freedom [65]. In our nominal MINER $\nu$ A analysis we allow for 30% uncertainty on the background motivated by the amount of tuning performed on the original backgrounds. Note that the nominal background predictions in the MINER $\nu$ A analysis overpredicts the data before tuning, and that tuning parameters are measured at the 3% level [51]. We also perform a background-ignorant analysis in which we assume 100% uncertainty for the background normalization, which only changes our conclusions by less than a factor of two. This emphasizes the robustness of our MINER $\nu$ A bound, since the NP typically overshoots the low-number of events in the sideband.

Our CHARM-II analysis is mostly based on Fig. 1 of [52]. This sample is shown as a function of  $E\theta^2$  and does not have any cuts on  $dE/dx$ . The new physics signal lies mostly in a region with small  $E\theta^2$ . Thus, we constrain backgrounds using the data from  $30 < E\theta^2 < 60$  MeV rad<sup>2</sup>. This sideband measurement constrains the normalization of the backgrounds in the signal region at the level of 3%. The extrapolation of the shape of the background to the signal region introduces the largest uncertainty in our analysis. For this reason, we raise the uncertainty of the background normalization from 3% to a conservative 10% when setting the limits. Flux uncertainties are assumed to be 4% [66], and are applicable to the new-physics signal,  $\nu - e$  scattering prediction, and backgrounds. Our  $\chi^2$  test is similar to the one used in the MINER $\nu$ A analysis and carries normalization nuisance parameters for the background and flux predictions. Uncertainties in the  $\nu - e$  scattering cross sections are expected to be sub-dominant and are neglected in the analysis [67].

A few comments on the MiniBooNE fit are in order. First, we have performed our own fit to the MiniBooNE energy spectrum using the data release from [5], and our results agree reasonably well with those of [45]. Second, it should be noted, that the data release only contains information about the neutrino energy and baseline distance.

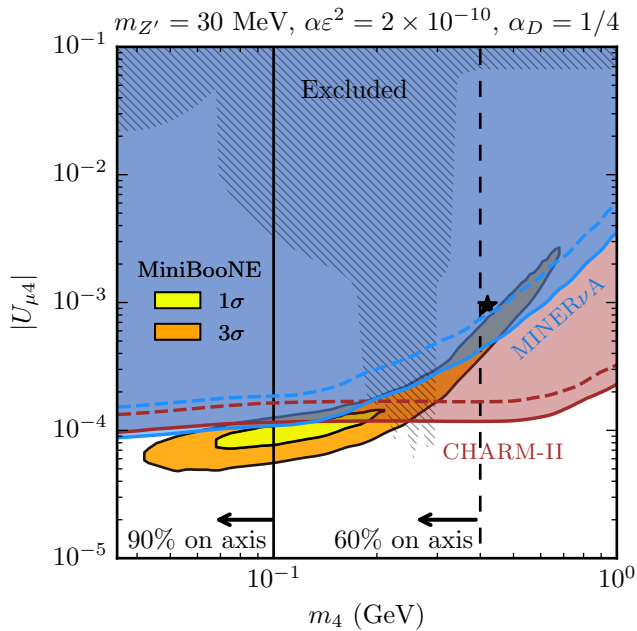


FIG. 3. *New constraints on mass generation model as a MiniBooNE explanation.* The MiniBooNE region of interest from [45], only fitted to the energy distribution, is shown as closed yellow (orange) regions for one (three) sigma C.L. The benchmark point, chosen to provide a good angular distribution fit, is shown as a black star. Exclusion from heavy neutrino searches is shown as a hatched background. Our new constraints at 90% C.L. using MINER $\nu$ A are shown in blue for our nominal 30% background normalization uncertainty (solid) and conservative case of 100% background uncertainty (dashed). Our CHARM-II bound is shown in red-cherry, where the 3% background normalization from the sideband is shown as a solid curve and the conservative 10% case as a dashed curve. The solid vertical black line at 100 MeV signals the point where 90% of NP events lie in the most forward bin in the MB angular distribution, and the dashed one where 60% of events do so. Other relevant assumed parameters are shown above the plot; changing them does not change our conclusion.

This makes the data release suitable for studying oscillation phenomena. However, for the models we consider, the re-weighting can only be performed approximately, as the angular information is needed to re-weight the quasi-elastic to the NP cross sections. Thus a proper analysis can only be performed if true and reconstructed electron angles and energies per simulated event are given.

**Results and conclusions** – The resulting limits at 90% confidence level (CL) in the  $|U_{\mu 4}|$  vs  $m_4$  plane are shown in Fig. 3, together with the MiniBooNE fit from [45]. We have chosen the same values of  $\varepsilon$ ,  $\alpha_D$ , and  $m_{Z'}$  as used in [45] for comparison. We note that the MiniBooNE event rate scales identically to our signal rate in all the couplings, and dependence of our bounds on  $m_{Z'}$  is sub-leading due to the large  $Q^2$  involved. This implies that changing the values of these parameters does

not modify the overall conclusions of our work. In addition, one can only lower the value of  $m_{Z'}$  to around 10 MeV before hitting beam dump constraints [68]. On the other hand, for this realization of the model, larger  $m_{Z'}$  implies larger values of  $m_4$ , increasing the tension between the MiniBooNE fit and our bounds. Our results from MINER $\nu$ A and CHARM-II are compatible given that they impose similar constraints for  $m_4 \lesssim 200$  MeV. For larger masses, the kinematics of the signal becomes less forward and the production thresholds start being important. This explains the up-turns visible in our bounds, where we observe it first MINER $\nu$ A and later in CHARM-II as we increase  $m_4$ , since CHARM-II has higher beam energy and the neutrino flux peaks at approximately 20 GeV.

The preferred region of [45] results from doing an energy-spectrum only fit to the MB data. This neglects the angular distribution of the MB excess. The preferred region of this energy-only fit is excluded by our analysis for masses of  $m_4$  greater than  $\approx 250$  MeV. As was recently pointed out in [69], reasonable angular distribution of new physics explanations of the MB excess requires hundreds of MeV NP particles. Since the MB data released do not provide the correlation between angle and energy and their associated systematics, a rigorous assessment of the tension is hard to quantify. The angular distribution of observed excess contains  $\approx 50\%$  of the events in the most forward bin, with a statistical uncorrelated uncertainty of 5% on this quantity. We use this information and our calculation of the angular distribution of the NP events from our dedicated MC to give an assessment of the tension in this observable. We draw a vertical line at  $m_4 = 100$  MeV, where 90% of the NP events would lie in the most forward bin and a dashed line at 60%. This 60% line, as expected, is close to the benchmark point of [46]. This consideration suggest that our analysis can rule out the model more significantly than by just comparing the energy-only fit preferred region and our curves.

In the near future, the MINER $\nu$ A medium-energy results on neutrino-electron scattering will be available. With the increase in energy, we estimate that it can improve the probe significantly if backgrounds, which are also rising, are well understood. This class of analyses will thus greatly benefit from improved calculations and measurements of coherent  $\pi^0$  production and single-photon emitting processes. This is particularly important if an excess is observed in these channels. A complementary result can also be obtained by measuring this process in NO $\nu$ A, which will sample a different kinematic regime as its off-axis beam peaks at lower energies and expects less NC $\pi^0$  events per ton. Interestingly, we note that this class of BSM signatures could be lurking in current measurements of  $\pi^0$  production, *e.g.*, at MINOS [70] and MINER $\nu$ A [71]. The latter measurement observes a significant excess of diffractive events which are abundant in similar realizations of this NP model [47]. To summarize, a variety of measurements are underway to further



lay siege to this explanation of the MB observation and, simultaneously, start probing testable neutrino mass generation models, as well as other similar NP signatures. It is clear that understanding neutrino cross sections will be crucial as we move forward.

### ACKNOWLEDGEMENTS

We thank Janet Conrad, Kareem Farrag, Alberto Gago, Gordan Krnjaic, Trung Le, Pedro Machado, Kevin McFarland, and Jorge Morfin for useful discussions, and Jean DeMerit for carefully proofreading our work. The authors would like to thank Fermilab for the hospitality at the initial stages of this project. Also, the au-

thors would like to thank Fermilab Theory Group and the CERN Theory Neutrino Platform for organizing the conference “Physics Opportunities in the Near DUNE Detector Hall,” which was essential to the completion of this work. CAA would especially like to thank Fermilab Center for Neutrino Physics summer visitor program for funding his visit. MH’s work was supported by Conselho Nacional de Ciência e Tecnologia (CNPq). CAA is supported by U.S. National Science Foundation (NSF) grant No. PHY-1801996. This document was prepared by YDT using the resources of the Fermi National Accelerator Laboratory (Fermilab), a U.S. Department of Energy, Office of Science, HEP User Facility. Fermilab is managed by Fermi Research Alliance, LLC (FRA), acting under Contract No. DE-AC02-07CH11359.

- 
- [1] Ivan Esteban, M. C. Gonzalez-Garcia, Alvaro Hernandez-Cabezudo, Michele Maltoni, and Thomas Schwetz, “Global analysis of three-flavour neutrino oscillations: synergies and tensions in the determination of  $\theta_{23}$ ,  $\delta_{CP}$ , and the mass ordering,” (2018), [arXiv:1811.05487 \[hep-ph\]](#).
- [2] C. Athanassopoulos *et al.* (LSND), “Evidence for anti-muon-neutrino  $\rightarrow$  anti-electron-neutrino oscillations from the LSND experiment at LAMPF,” *Phys. Rev. Lett.* **77**, 3082–3085 (1996), [arXiv:nucl-ex/9605003 \[nucl-ex\]](#).
- [3] A. Aguilar-Arevalo *et al.* (LSND), “Evidence for neutrino oscillations from the observation of anti-neutrino(electron) appearance in a anti-neutrino(muon) beam,” *Phys. Rev.* **D64**, 112007 (2001), [arXiv:hep-ex/0104049 \[hep-ex\]](#).
- [4] A. A. Aguilar-Arevalo *et al.* (MiniBooNE), “A Search for electron neutrino appearance at the  $\Delta m^2 \sim 1\text{eV}^2$  scale,” *Phys. Rev. Lett.* **98**, 231801 (2007), [arXiv:0704.1500 \[hep-ex\]](#).
- [5] A. A. Aguilar-Arevalo *et al.* (MiniBooNE), “Observation of a Significant Excess of Electron-Like Events in the MiniBooNE Short-Baseline Neutrino Experiment,” (2018), [arXiv:1805.12028 \[hep-ex\]](#).
- [6] LEP Electroweak Working Group (ALEPH, CDF, D0, DELPHI, L3, OPAL, SLD, LEP Electroweak Working Group, Tevatron Electroweak Working Group, SLD Electroweak and Heavy Flavour Groups), “Precision Electroweak Measurements and Constraints on the Standard Model,” (2010), [arXiv:1012.2367 \[hep-ex\]](#).
- [7] Collin, G. H. and Argüelles, C. A. and Conrad, J. M. and Shaevitz, M. H., “First Constraints on the Complete Neutrino Mixing Matrix with a Sterile Neutrino,” (2016), [arXiv:1607.00011 \[hep-ph\]](#).
- [8] Francesco Capozzi, Carlo Giunti, Marco Laveder, and Antonio Palazzo, “Joint short- and long-baseline constraints on light sterile neutrinos,” *Phys. Rev.* **D95**, 033006 (2017), [arXiv:1612.07764 \[hep-ph\]](#).
- [9] Mona Dentler, Álvaro Hernández-Cabezudo, Joachim Kopp, Pedro A. N. Machado, Michele Maltoni, Ivan Martinez-Soler, and Thomas Schwetz, “Updated Global Analysis of Neutrino Oscillations in the Presence of eV-Scale Sterile Neutrinos,” *JHEP* **08**, 010 (2018), [arXiv:1803.10661 \[hep-ph\]](#).
- [10] A. A. Aguilar-Arevalo *et al.* (MiniBooNE), “Unexplained Excess of Electron-Like Events From a 1-GeV Neutrino Beam,” *Phys. Rev. Lett.* **102**, 101802 (2009), [arXiv:0812.2243 \[hep-ex\]](#).
- [11] A. A. Aguilar-Arevalo *et al.* (MiniBooNE), “A Combined  $\nu_\mu \rightarrow \nu_e$  and  $\bar{\nu}_\mu \rightarrow \bar{\nu}_e$  Oscillation Analysis of the MiniBooNE Excesses,” (2012) [arXiv:1207.4809 \[hep-ex\]](#).
- [12] Richard J. Hill, “On the single photon background to  $\nu_e$  appearance at MiniBooNE,” *Phys. Rev.* **D84**, 017501 (2011), [arXiv:1002.4215 \[hep-ph\]](#).
- [13] Hitoshi Murayama and T. Yanagida, “LSND, SN1987A, and CPT violation,” *Phys. Lett.* **B520**, 263–268 (2001), [arXiv:hep-ph/0010178 \[hep-ph\]](#).
- [14] Alessandro Strumia, “Interpreting the LSND anomaly: Sterile neutrinos or CPT violation or...?” *Phys. Lett.* **B539**, 91–101 (2002), [arXiv:hep-ph/0201134 \[hep-ph\]](#).
- [15] G. Barenboim, L. Borissov, and Joseph D. Lykken, “CPT violating neutrinos in the light of KamLAND,” (2002), [arXiv:hep-ph/0212116 \[hep-ph\]](#).
- [16] M. C. Gonzalez-Garcia, M. Maltoni, and T. Schwetz, “Status of the CPT violating interpretations of the LSND signal,” *Phys. Rev.* **D68**, 053007 (2003), [arXiv:hep-ph/0306226 \[hep-ph\]](#).
- [17] V. Barger, D. Marfatia, and K. Whisnant, “LSND anomaly from CPT violation in four neutrino models,” *Phys. Lett.* **B576**, 303–308 (2003), [arXiv:hep-ph/0308299 \[hep-ph\]](#).
- [18] Michel Sorel, Janet M. Conrad, and Michael Shaevitz, “A Combined analysis of short baseline neutrino experiments in the (3+1) and (3+2) sterile neutrino oscillation hypotheses,” *Phys. Rev.* **D70**, 073004 (2004), [arXiv:hep-ph/0305255 \[hep-ph\]](#).
- [19] Gabriela Barenboim and Nick E. Mavromatos, “CPT violating decoherence and LSND: A Possible window to Planck scale physics,” *JHEP* **01**, 034 (2005), [arXiv:hep-ph/0404014 \[hep-ph\]](#).
- [20] Kathryn M. Zurek, “New matter effects in neutrino oscillation experiments,” *JHEP* **10**, 058 (2004), [arXiv:hep-ph/0405141 \[hep-ph\]](#).
- [21] David B. Kaplan, Ann E. Nelson, and Neal Weiner, “Neutrino oscillations as a probe of dark energy,” *Phys. Rev. Lett.* **93**, 091801 (2004), [arXiv:hep-ph/0401099 \[hep-ph\]](#).

- [22] Heinrich Pas, Sandip Pakvasa, and Thomas J. Weiler, “Sterile-active neutrino oscillations and shortcuts in the extra dimension,” *Phys. Rev.* **D72**, 095017 (2005), [arXiv:hep-ph/0504096 \[hep-ph\]](#).
- [23] Andre de Gouvêa and Yuval Grossman, “A Three-flavor, Lorentz-violating solution to the LSND anomaly,” *Phys. Rev.* **D74**, 093008 (2006), [arXiv:hep-ph/0602237 \[hep-ph\]](#).
- [24] Thomas Schwetz, “LSND versus MiniBooNE: Sterile neutrinos with energy dependent masses and mixing?” *JHEP* **02**, 011 (2008), [arXiv:0710.2985 \[hep-ph\]](#).
- [25] Yasaman Farzan, Thomas Schwetz, and Alexei Yu Smirnov, “Reconciling results of LSND, MiniBooNE and other experiments with soft decoherence,” *JHEP* **07**, 067 (2008), [arXiv:0805.2098 \[hep-ph\]](#).
- [26] Sebastian Hollenberg, Octavian Micu, Heinrich Pas, and Thomas J. Weiler, “Baseline-dependent neutrino oscillations with extra-dimensional shortcuts,” *Phys. Rev.* **D80**, 093005 (2009), [arXiv:0906.0150 \[hep-ph\]](#).
- [27] Ann E. Nelson, “Effects of CP Violation from Neutral Heavy Fermions on Neutrino Oscillations, and the LSND/MiniBooNE Anomalies,” *Phys. Rev.* **D84**, 053001 (2011), [arXiv:1010.3970 \[hep-ph\]](#).
- [28] Evgeny Akhmedov and Thomas Schwetz, “MiniBooNE and LSND data: Non-standard neutrino interactions in a (3+1) scheme versus (3+2) oscillations,” *JHEP* **10**, 115 (2010), [arXiv:1007.4171 \[hep-ph\]](#).
- [29] Jorge S. Diaz and V. Alan Kostelecky, “Three-parameter Lorentz-violating texture for neutrino mixing,” *Phys. Lett.* **B700**, 25–28 (2011), [arXiv:1012.5985 \[hep-ph\]](#).
- [30] Yang Bai, Ran Lu, Sida Lu, Jordi Salvado, and Ben A. Stefanek, “Three Twin Neutrinos: Evidence from LSND and MiniBooNE,” *Phys. Rev.* **D93**, 073004 (2016), [arXiv:1512.05357 \[hep-ph\]](#).
- [31] C. Giunti and E. M. Zavatin, “Appearance–disappearance relation in  $3 + N_s$  short-baseline neutrino oscillations,” *Mod. Phys. Lett.* **A31**, 1650003 (2015), [arXiv:1508.03172 \[hep-ph\]](#).
- [32] Jiajun Liao and Danny Marfatia, “Impact of nonstandard interactions on sterile neutrino searches at IceCube,” *Phys. Rev. Lett.* **117**, 071802 (2016), [arXiv:1602.08766 \[hep-ph\]](#).
- [33] D. K. Papoulias and T. S. Kosmas, “Impact of Non-standard Interactions on Neutrino-Nucleon Scattering,” *Adv. High Energy Phys.* **2016**, 1490860 (2016), [arXiv:1611.05069 \[hep-ph\]](#).
- [34] Zander Moss, Marjon H. Moulai, Carlos A. Argüelles, and Janet M. Conrad, “Exploring a nonminimal sterile neutrino model involving decay at IceCube,” *Phys. Rev.* **D97**, 055017 (2018), [arXiv:1711.05921 \[hep-ph\]](#).
- [35] Marcela Carena, Ying-Ying Li, Camila S. Machado, Pedro A. N. Machado, and Carlos E. M. Wagner, “Neutrinos in Large Extra Dimensions and Short-Baseline  $\nu_e$  Appearance,” (2017), [arXiv:1708.09548 \[hep-ph\]](#).
- [36] Jiajun Liao, Danny Marfatia, and Kerry Whisnant, “MiniBooNE, MINOS+ and IceCube data imply a baroque neutrino sector,” (2018), [arXiv:1810.01000 \[hep-ph\]](#).
- [37] S. N. Gninenko, “The MiniBooNE anomaly and heavy neutrino decay,” *Phys. Rev. Lett.* **103**, 241802 (2009), [arXiv:0902.3802 \[hep-ph\]](#).
- [38] Sergei N. Gninenko, “A resolution of puzzles from the LSND, KARMEN, and MiniBooNE experiments,” *Phys. Rev.* **D83**, 015015 (2011), [arXiv:1009.5536 \[hep-ph\]](#).
- [39] Claudio Dib, Juan Carlos Helo, Sergey Kovalenko, and Ivan Schmidt, “Sterile neutrino decay explanation of LSND and MiniBooNE anomalies,” *Phys. Rev.* **D84**, 071301 (2011), [arXiv:1105.4664 \[hep-ph\]](#).
- [40] David McKeen and Maxim Pospelov, “Muon Capture Constraints on Sterile Neutrino Properties,” *Phys. Rev.* **D82**, 113018 (2010), [arXiv:1011.3046 \[hep-ph\]](#).
- [41] Manuel Masip, Pere Masjuan, and Davide Meloni, “Heavy neutrino decays at MiniBooNE,” *JHEP* **01**, 106 (2013), [arXiv:1210.1519 \[hep-ph\]](#).
- [42] Manuel Masip and Pere Masjuan, “Heavy-neutrino decays at neutrino telescopes,” *Phys. Rev.* **D83**, 091301 (2011), [arXiv:1103.0689 \[hep-ph\]](#).
- [43] S. N. Gninenko, “New limits on radiative sterile neutrino decays from a search for single photons in neutrino interactions,” *Phys. Lett.* **B710**, 86–90 (2012), [arXiv:1201.5194 \[hep-ph\]](#).
- [44] Gabriel Magill, Ryan Plestid, Maxim Pospelov, and Yu-Dai Tsai, “Dipole portal to heavy neutral leptons,” (2018), [arXiv:1803.03262 \[hep-ph\]](#).
- [45] Enrico Bertuzzo, Sudip Jana, Pedro A. N. Machado, and Renata Zukanovich Funchal, “A Dark Neutrino Portal to Explain MiniBooNE,” (2018), [arXiv:1807.09877 \[hep-ph\]](#).
- [46] Enrico Bertuzzo, Sudip Jana, Pedro A. N. Machado, and Renata Zukanovich Funchal, “Neutrino Masses and Mixings Dynamically Generated by a Light Dark Sector,” (2018), [arXiv:1808.02500 \[hep-ph\]](#).
- [47] Peter Ballett, Silvia Pascoli, and Mark Ross-Lonergan, “U(1)’ mediated decays of heavy sterile neutrinos in MiniBooNE,” (2018), [arXiv:1808.02915 \[hep-ph\]](#).
- [48] L. B. Auerbach *et al.* (LSND), “Measurement of electron - neutrino - electron elastic scattering,” *Phys. Rev.* **D63**, 112001 (2001), [arXiv:hep-ex/0101039 \[hep-ex\]](#).
- [49] M. Deniz *et al.* (TEXONO), “Measurement of Nu(e)-bar -Electron Scattering Cross-Section with a CsI(Tl) Scintillating Crystal Array at the Kuo-Sheng Nuclear Power Reactor,” *Phys. Rev.* **D81**, 072001 (2010), [arXiv:0911.1597 \[hep-ex\]](#).
- [50] G. Bellini *et al.*, “Precision measurement of the  $7\text{Be}$  solar neutrino interaction rate in Borexino,” *Phys. Rev. Lett.* **107**, 141302 (2011), [arXiv:1104.1816 \[hep-ex\]](#).
- [51] Jaewon Park, *Neutrino-Electron Scattering in MINERvA for Constraining the NuMI Neutrino Flux*, Ph.D. thesis, U. Rochester (2013).
- [52] P. Vilain *et al.* (CHARM-II), “Precision measurement of electroweak parameters from the scattering of muon-neutrinos on electrons,” *Phys. Lett.* **B335**, 246–252 (1994).
- [53] Maxim Pospelov and Yu-Dai Tsai, “Light scalars and dark photons in Borexino and LSND experiments,” *Phys. Lett.* **B785**, 288–295 (2018), [arXiv:1706.00424 \[hep-ph\]](#).
- [54] Manfred Lindner, Farinaldo S. Queiroz, Werner Rodejohann, and Xun-Jie Xu, “Neutrino-electron scattering: general constraints on  $Z'$  and dark photon models,” *JHEP* **05**, 098 (2018), [arXiv:1803.00060 \[hep-ph\]](#).
- [55] Gabriel Magill, Ryan Plestid, Maxim Pospelov, and Yu-Dai Tsai, “Millicharged particles in neutrino experiments,” (2018), [arXiv:1806.03310 \[hep-ph\]](#).
- [56] J. Park *et al.* (MINERvA), “Measurement of Neutrino Flux from Neutrino-Electron Elastic Scattering,” *Phys. Rev.* **D93**, 112007 (2016), [arXiv:1512.07699 \[physics.ins-det\]](#).

- [57] Edgar Valencia-Rodriguez, *Neutrino - Electron Scattering in MINERvA for Constraint NuMI Flux at Medium*, Ph.D. thesis, Guanajuato U. (2016).
- [58] K. De Winter *et al.* (CHARM-II), “A Detector for the Study of Neutrino - Electron Scattering,” *Nucl. Instrum. Meth.* **A278**, 670 (1989).
- [59] D. Geiregat *et al.* (CHARM-II), “Calibration and performance of the CHARM-II detector,” *Nucl. Instrum. Meth.* **A325**, 92–108 (1993).
- [60] Eung Jin Chun, Jong-Chul Park, and Stefano Scopel, “Dark matter and a new gauge boson through kinetic mixing,” *JHEP* **02**, 100 (2011), [arXiv:1011.3300 \[hep-ph\]](https://arxiv.org/abs/1011.3300).
- [61] Stephen Parke and Mark Ross-Lonergan, “Unitarity and the Three Flavour Neutrino Mixing Matrix,” (2015), [arXiv:1508.05095 \[hep-ph\]](https://arxiv.org/abs/1508.05095).
- [62] L. Aliaga *et al.* (MINERvA), “Design, Calibration, and Performance of the MINERvA Detector,” *Nucl. Instrum. Meth.* **A743**, 130–159 (2014), [arXiv:1305.5199 \[physics.ins-det\]](https://arxiv.org/abs/1305.5199).
- [63] Berger, M.J. and Coursey, J.S. and Zucker, M.A. and Chang, J., “<https://dx.doi.org/10.18434/T4NC7P>”.
- [64] W. R. Leo, *Techniques for Nuclear and Particle Physics Experiments: A How to Approach* (1987).
- [65] M. Tanabashi *et al.* (Particle Data Group), “Review of Particle Physics,” *Phys. Rev.* **D98**, 030001 (2018).
- [66] J. V. Allaby *et al.* (CHARM), “Total Cross-sections of Charged Current Neutrino and Anti-neutrino Interactions on Isoscalar Nuclei,” *Z. Phys.* **C38**, 403–410 (1988).
- [67] Andre de Gouvea and James Jenkins, “What can we learn from neutrino electron scattering?” *Phys. Rev.* **D74**, 033004 (2006), [arXiv:hep-ph/0603036 \[hep-ph\]](https://arxiv.org/abs/hep-ph/0603036).
- [68] Martin Bauer, Patrick Foldenauer, and Joerg Jaeckel, “Hunting All the Hidden Photons,” *JHEP* **07**, 094 (2018), [arXiv:1803.05466 \[hep-ph\]](https://arxiv.org/abs/1803.05466).
- [69] Johnathon R. Jordan, Yonatan Kahn, Gordan Krnjaic, Matthew Moschella, and Joshua Spitz, “Severe Constraints on New Physics Explanations of the MiniBooNE Excess,” (2018), [arXiv:1810.07185 \[hep-ph\]](https://arxiv.org/abs/1810.07185).
- [70] P. Adamson *et al.* (MINOS), “Measurement of single  $\pi^0$  production by coherent neutral-current  $\nu$  Fe interactions in the MINOS Near Detector,” *Phys. Rev.* **D94**, 072006 (2016), [arXiv:1608.05702 \[hep-ex\]](https://arxiv.org/abs/1608.05702).
- [71] J. Wolcott *et al.* (MINERvA), “Evidence for Neutral-Current Diffractive  $\pi^0$  Production from Hydrogen in Neutrino Interactions on Hydrocarbon,” *Phys. Rev. Lett.* **117**, 111801 (2016), [arXiv:1604.01728 \[hep-ex\]](https://arxiv.org/abs/1604.01728).